

Fig. 2 Equivalence of solutions for constant and varying edge temperatures.

and Eq. (6) becomes

$$\frac{\partial \bar{T}}{\partial t^*} = 4 + \frac{1}{r^*} \frac{\partial \bar{T}}{\partial r^*} + \frac{1}{r^*} \frac{\partial X}{\partial r^*} + \frac{\partial^2 \bar{T}}{\partial r^{*2}} + \frac{\partial^2 X}{\partial r^{*2}} \quad (9)$$

After separating variables and utilizing the transformed boundary conditions, the solution of Eq. (9) becomes

$$T^*(r^*, t^*) = A J_0(\lambda_j r^*) e^{-\lambda_j^2 t^*} + 1 - r^{*2} \quad (10)$$

Further application of the boundary conditions, integration, and simplification results in

$$T^*(r^*, t^*) = 2 \sum_{j=1}^{\infty} \frac{J_0(\lambda_j r^*)}{[J_1(\lambda_j)]^2} e^{-\lambda_j^2 t^*} \left[-\frac{4}{\lambda_j^3} J_1(\lambda_j) \right] + 1 - r^{*2} \quad (11)$$

Equation (11) is the complete solution for the case of uniform edge temperature. For complete details of all mathematical steps, the reader should consult Ref. 5. When the edge temperature becomes a function of time however, with Eq. (9) remaining the same, $T(r=R, t) = f(t)$, the new original boundary condition, is transformed to $T^*(r^*=1, t^*) = \bar{T}(r^*=1, t^*)$, with the other transformed boundary conditions remaining the same. By Duhamel's theorem, which basically allows the transient solution to be expressed in terms of the steady-state solution as defined by Eq. (11), it is possible to express the exponential portion of Eq. (11), the only portion that changes, as follows:

$$\bar{T}_N(r^*, t^*) = F(+0) \bar{T}(r^*, t^*) + \int_0^{t^*} F'(t-\tau) \bar{T}(r^*, t^*) d\tau \quad (12)$$

$F(+0)$ is the edge temperature function evaluated at time = 0 while $F'(t-\tau)$ is the first derivative of that same function. The integration thus required is with respect to the time variable and is, generally, of the form

$$\int_0^{t^*} e^{-\lambda_j^2 t^*} (B + 2Ct^* + 3Dt^{*2} + \dots) dt^* \quad (13)$$

where a polynomial edge temperature function has been assumed.

Thus Duhamel's theorem provides a very useful tool with which to solve the case of varying edge temperature once the solution for a uniform edge reference temperature has been established. The following curve provides a numerical example, in lieu of a classical mathematical proof, that the two solutions

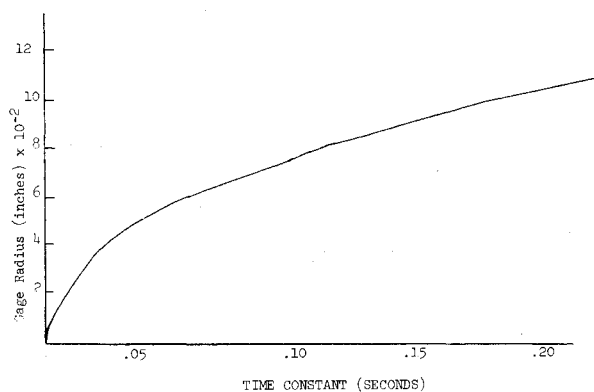


Fig. 3 Gage response capability.

are equivalent. The edge temperature function, based on data by Laganelli,³ is given by $f(t) = 79.86 + 5.874t$.

Conclusions

The result shows that even though the edge temperature varies with time, the difference between the center and edge temperature remains constant; thus the gage correctly measures heat flux input through both transient and steady-state sink temperatures. For small values of time, the exponential time function dominates the solution, and it is important to carry more terms in the Bessel summation. As time increases, however, the exponential quickly fades as does the contribution of each succeeding Bessel term. Unlike Fourier summations, only five terms of the Bessel series, with the number decreasing with increasing time, gave very good accuracy. Small gages are controlled by the transient part of the eigenvalues (λ_j 's), while the Bessel portion, as defined by the same eigenvalues, controls the geometry. Accuracy, then, does not suffer as the sink temperature varies with time, but does depend on a gage response at least as fast as the edge temperature is changing. The following curve shows time constant vs gage radius, time constant being defined as that time at which temperature reaches 63% of its steady-state value.

References

- Gardon, R., "An Instrument for the Direct Measurement of Intense Thermal Radiation," *The Review of Scientific Instruments*, May 1953, pp. 366-370.
- Coffin, G. R., "A Study of Miniature Heat Flux Meters," M.S. thesis, 1964, Brigham Young University, Provo, Utah.
- Laganelli, A. L. and Martellucci, A., "The Effect of Mass Addition Around a Blunt Nose on Flow Properties and Vehicle Cooling," *General Electric Technical Information Series*, 72SD250, Nov. 1972, General Electric Co., Valley Forge, Pa.
- Martellucci, A., Hahn, J., and Laganelli, A. L., "Effect of Mass Addition and Angle-of-Attack On the Turbulent Boundary Layer Characteristics Of a Slender Cone," *General Electric Technical Information Series*, 73SD210, April 1973, General Electric Co., Valley Forge, Pa.
- Kita, J. P. and Laganelli, A. L., "On the Behavior of Gardon Type Heat Gages with Transient Boundary Conditions," *General Electric Technical Information Series*, 74SD207, March 1974, General Electric Co., Valley Forge, Pa.

Minimum Heat Transfer Limit in Simple and Gas-Loaded Heat Pipes

A. R. ROHANI* AND C. L. TIEN†

University of California, Berkeley, Calif.

Introduction

THE operational limits of heat pipes in terms of maximum heat flux have been studied by many investigators.¹⁻⁴ Some limits have their origins in the vapor flow behavior such as the sonic and the viscous limits,^{3,4} while others such as the boiling, capillary, and entrainment limits are not directly related to vapor flow. The minimum heat transfer limit discussed here is mainly a result of the vapor flow phenomenon. It is defined as the lowest rate of heat transfer through the heat pipe below which there no longer exists a section with a uniform temperature higher than the

Received August 1, 1974; revision received September 23, 1974.

Index categories: Viscous Nonboundary-Layer Flow; Heat Conduction; Thermal Modeling and Experimental Thermal Simulation.

* Department of Mechanical Engineering, currently with the University of Teheran, Iran.

† Professor of Mechanical Engineering, Associate Fellow AIAA.

condenser ambient temperature along the heat pipe condenser section, and the temperature decreases continuously in that section. When the heat transfer rate is lower than this minimum in a heat pipe, energy is transferred along the system by heat conduction through the heat pipe wall and liquid-wick matrix as well as the vapor, and the heat pipe wall ceases to function as an effective heat transfer device as intended. In such a situation, a relatively large vapor pressure drop occurs along the heat pipe. This pressure drop in simple heat pipes is mainly due to viscous effects, while in gas-loaded heat pipes it can also be a result of the increasing volume and partial pressure of the noncondensable gas in the vapor-gas region of the system. When the noncondensable gas enters the evaporator section, a large-scale mixing of vapor and gas will take place.

To demonstrate the existence of the minimum heat transfer limit in heat pipe operation, the partial differential conservation equations of mass, momentum, energy and species developed for studying the normal operation of the simple and gas-loaded heat pipes^{6,7} have been solved under specific conditions for a simple sodium heat pipe and a sodium-argon gas-loaded heat pipe. By lowering the rate of heat transfer through the system the minimum heat transfer rate is established in each case, and the axial temperature profiles obtained by neglecting the axial heat conduction through the heat pipe wall and the liquid-wick matrix as the heat pipe approaches the above limit are presented.

General Considerations

The minimum heat transfer limit in heat pipes is encountered in experiments when the rate of heat input to the system has to be raised above a certain level before a nearly uniform temperature can be established along the heat pipe. This and other similar observations reveal that below certain heat transfer rates the highly conductive heat pipe wall transmits a major portion of the total heat input to the heat pipe, and the vapor contributes little to the heat transfer process. In other words, conduction rather than convection becomes the dominant heat transfer mode in the heat pipe. A qualitative description of this minimum heat transfer limit has also been given by Cotter⁸ in relation to heat pipe start-up dynamics. Busse⁴ has also indicated the existence of this phenomenon.

In order to compare the relative magnitude of the heat transfer rate by conduction to that by convection along the heat pipe, the partial differential conservation equations of mass, momentum, energy and species for the simple and the gas-loaded heat pipes are solved numerically for the operating conditions near their minimum heat transfer limits. To demonstrate clearly the significant role of vapor flow, the present calculation assumes negligible energy transport through the heat pipe wall and the liquid-wick matrix. This, however, is not to minimize the importance of the axial heat conduction through the heat pipe wall and the liquid-wick matrix, especially in the operating conditions near the minimum heat transfer limit because of the large temperature gradients. A method has been indicated⁷

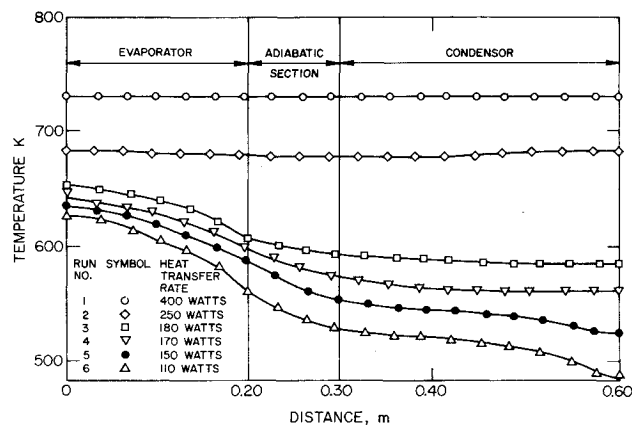


Fig. 1 Axial temperature variation along the vapor-liquid interface of the simple sodium heat pipe.

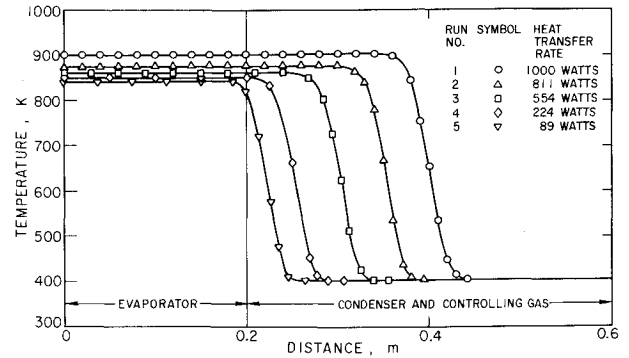


Fig. 2 Axial temperature variation along the vapor-liquid interface of the sodium-argon gas-loaded heat pipe.

regarding how to incorporate the axial heat conduction through the heat pipe wall and the liquid-wick matrix into calculation in actual determination of the minimum heat transfer limit.

The governing differential equations for the simple heat pipe consist of the mass, momentum and energy conservation equations. For the gas-loaded heat pipe, the species conservation equation is also included. For the numerical method of solution employed here, the mass and momentum conservation equations are expressed in terms of stream function and vorticity. In cylindrical coordinates they have the following general form:

$$a_{\phi} \left\{ \frac{\partial}{\partial x} \left(\phi \frac{\partial \psi}{\partial r} \right) \right\} - a_{\phi} \left\{ \frac{\partial}{\partial r} \left(\phi \frac{\partial \psi}{\partial x} \right) \right\} - \frac{\partial}{\partial x} \left\{ b_{\phi} r \frac{\partial}{\partial x} (c_{\phi} \phi) \right\} - \frac{\partial}{\partial r} \left\{ b_{\phi} r \frac{\partial}{\partial r} (c_{\phi} \phi) \right\} + r d_{\phi} = 0$$

where ϕ represents any of the following variables: vorticity, stream function, enthalpy or mass composition; ψ is stream function and a, b, c and d are functions of the variable ϕ .⁹ The boundary conditions to these equations for simple and gas-loaded heat pipes and the over-all energy, mass and species constraints on them have been extensively discussed elsewhere.^{6,7} The equations are solved numerically by using the upwind method of differencing.⁹ The results are obtained by carefully following the special solution procedures given for the simple and gas-loaded heat pipes.^{6,7}

Results and Discussion

A cylindrical heat pipe with sodium as the working fluid operating in a certain temperature range is selected in such a way that while the operating pressure inside the system is low, the pressure and temperature drops along the pipe are relatively large.⁶ Six cases of simple heat pipe operation at heat transfer rates above, near and below the minimum heat transfer limit are analyzed. Table 1 gives the primary information about the six

Table 1 Primary information on the six simple sodium heat pipe cases

Case No.	$T_{ac}(K)$	$T_{ae}(K)$	$T_o(K)$	$r_o(m)$	$L(m)$	H_c ($Wm^{-2}K^{-1}$)	H_e ($Wm^{-2}K^{-1}$)
1	400	820	750	0.025	0.6	24.0	182.0
2	400	760	700	0.025	0.6	18.0	133.0
3	400	700	650	0.025	0.6	17.0	127.0
4	400	690	640	0.025	0.6	16.7	119.0
5	400	680	630	0.025	0.6	15.4	106.0
6	400	650	590	0.025	0.6	13.7	64.7

cases, while Fig. 1 shows the axial temperature distribution at the heat pipe vapor-liquid interface of the six cases. The symbols used in Table 1 are defined⁹ as follows: T_{ac} the ambient condenser temperature, T_{ae} the ambient evaporator temperature, T_o the operating vapor temperature, r_o the vapor core radius, L the heat pipe length, and H_c and H_e the over-all heat

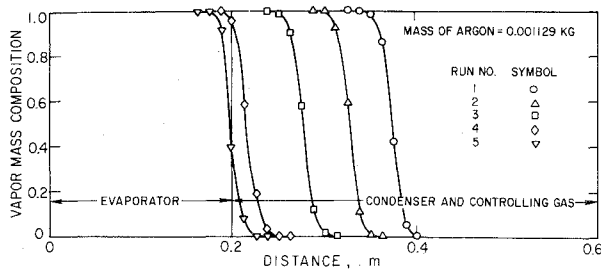


Fig. 3 Axial sodium-vapor mass composition variation along the vapor-liquid interface of the gas-loaded heat pipe.

transfer coefficients in condenser and evaporator respectively. From these results, the minimum heat transfer rate for the heat pipe under study is found to be about 200 w, and at heat transfer rates below this level a continuous temperature drop occurs along the heat pipe.

Similar to the simple heat pipe case, a cylindrical heat pipe with sodium as the working fluid and argon as the controlling gas is selected for the analysis.⁷ Five cases of the sodium-argon gas-loaded heat pipe are analyzed. In these cases, the rate of heat transfer through the system is lowered in such a way that the constant mass of argon occupies an increasing length of the heat pipe condenser section and eventually enters the heat pipe evaporator section in Case No. 5. Table 2 gives the primary

Table 2 Primary information on the five sodium-argon gas-loaded heat pipe cases

Case No.	$T_{ac}(K)$	$T_{de}(K)$	$T_o(K)$	$r_o(m)$	$L(m)$	$H_c (Wm^{-2}K^{-1})$	$H_e (Wm^{-2}K^{-1})$
1	400	1000	900	0.025	0.6	32	159
2	400	944	873	0.025	0.6	32	159
3	400	905	859	0.025	0.6	32	159
4	400	870	848	0.025	0.6	32	159
5	400	851	842	0.025	0.6	32	159

information about the cases studied while Figs. 2 and 3 demonstrate the axial temperature and sodium vapor mass composition variations along the heat pipe vapor-liquid interface. The minimum heat transfer rate limit is about 250 watts here as demonstrated in Figs. 2 and 3. The profiles in Figs. 1–3 are obtained as mentioned before, by neglecting the axial heat conduction through the heat pipe wall and the liquid-wick matrix. Obviously, when this conduction contribution is taken into consideration, the minimum heat transfer limit will be much higher, and its importance in actual design consideration cannot be overlooked.

References

- Cotter, T. P., "Theory of Heat Pipes," Rept. LA-3246-MS, March 1965, Los Alamos Scientific Lab., Los Alamos, New Mex.
- Kemme, J. E., "Heat Pipe Design Considerations," Rept. LA-4221-MS, August 1966, Los Alamos Scientific Lab. Los Alamos, New Mex.
- Levy, E. K., "Theoretical Investigation of Heat Pipes Operating at Low Vapor Pressures," *Journal of Engineering for Industry*, Vol. 90, 1968, pp. 547–552.
- Busse, C. A., "Theory of the Ultimate Heat Transfer Limit of Cylindrical Heat Pipes," *International Journal of Heat and Mass Transfer*, Vol. 16, 1973, pp. 169–186.
- Marcus, B. D., Fleischman, C. L., and Edwards, D. K., "Diffusion Freeze-out in Gas-Loaded Heat Pipes," ASME Paper 72-WA/HT-33, 1972.
- Tien, C. L., and Rohani, A. R., "Analysis of the Effects of Vapor Pressure Drop on Heat Pipe Performance," *International Journal of Heat and Mass Transfer*, Vol. 17, 1974, pp. 61–67.
- Rohani, A. R., and Tien, C. L., "Steady Two-Dimensional Heat and Mass Transfer in the Vapor-Gas Region of a Gas-Loaded Heat Pipe," *Journal of Heat Transfer*, Vol. 95, 1973, pp. 337–382.
- Cotter, T. P., "Heat Pipe Startup Dynamics," 1967 IEEE Conference Record of the Thermionic Conversion Specialist Conference, 1967, pp. 344–348.
- Gosman, A. D., Pun, W. M., Runchal, A. K., Spalding, D. B., and Wolfstein, M., *Heat and Mass Transfer in Recirculating Flows*, Academic Press, New York, 1969.

ference Record of the Thermionic Conversion Specialist Conference, 1967, pp. 344–348.

⁹ Gosman, A. D., Pun, W. M., Runchal, A. K., Spalding, D. B., and Wolfstein, M., *Heat and Mass Transfer in Recirculating Flows*, Academic Press, New York, 1969.

Variable Time Step Method for Determining Plastic Stress Reflections from Boundaries

HYMAN GARNET* AND HARRY ARMENT†

Grumman Aerospace Corporation, Bethpage, N.Y.

IT is the purpose of this Note to call attention to the advantages of the use of a variable time step direct integration method, in conjunction with a finite element analysis, for obtaining accurate results for elasto-plastic wave propagation, including reflections from fixed boundaries.

Recently, increased interest has been shown in the application of finite element analyses to problems in structural dynamics. An important role in such procedures is the appropriate use of a direct integration method to handle the time dependence. The more popular schemes employed have been Houbolt's, Newmark-Beta, central difference, and Wilson's methods. These procedures have been surveyed in a number of publications, for example, by Nickell¹ and the present authors.² These procedures all involve the use of a constant time step.

The present authors applied a number of direct integration techniques to the finite element analysis of a rod experiencing elastic and elasto-plastic wave propagation effects, either from an applied step pulse, or from a constant velocity impact into a rigid barrier.² After completion of the investigation, it was concluded that constant time step procedures, while capable of being adjusted to converge to acceptable results, were inappropriate to many practical problems, in particular to the increasingly important area of crashworthiness. The problem of selecting a constant time step, which would lead to convergent results is computationally equivalent to "flying" a vehicle, crashing it, and analyzing it several times until a time step is found that produces satisfactory convergence. This need for duplication of analysis is eliminated by the use of variable time step procedures, in which the time step may be varied at different instants to reflect the dynamic behavior of the structure, i.e., the time increment is increased during a slowly varying portion of the response, and decreased during a rapidly varying portion of the response. Thus, stability, accuracy, and efficiency requirements are met by built-in procedures.

In this Note, the authors draw on results obtained by them in Ref. 1, and more recently, to support the feasibility of applying a variable time step procedure to finite element structural dynamic analysis. The procedure referred to is a Grumman-developed version of the modified Adams method.³ It has been applied to a variety of significant aerospace structural dynamics problems, for example, as listed in Refs. 4 and 5. Recently, the present authors have employed this variable time step procedure to obtain accurate predicted results for elasto-plastic wave propagation, including the case of waves reflected from boundaries. The method employs Taylor series expansions to obtain predictor-corrector expressions, truncated to difference form, of the solution to a first-order system of

Received July 31, 1974; revision received September 18, 1974.

Index category: Aircraft Structural Design (Including Loads).

* Research Scientist, Research Department.

† Head, Applied Mechanics Branch. Member AIAA.